Supporting Information

Distribution of Water in Pores of Periodic Mesoporous OrganoSilicates –

a Proton Solid State MAS NMR Study

V. S. Veena [a], Illath Kavya [b], Anish Lazar[c], C. P. Vinod[c], T. G. Ajithkumar[b], Sundaresan Jayanthi[a*]

[a]Department of Physics, Indian Institute of Space Science and Technology, Valiamala, Thiruvananthapuram 695 547, Kerala, India.

[b]Central NMR Facility and Physical and Materials Chemistry Division, CSIR-National Chemical Laboratory, Pune, Maharashtra, India.

[c]Catalysis and Inorganic Chemistry Division, CSIR-National Chemical Laboratory, Pune, Maharashtra, India.

*Author for correspondence: jayanthi.s@iist.ac.in

Phone number: +91 471 2568658; Fax No. +91 471 2568542

CONTENTS

Analysis of the PMO$_E$ proton spectrum

The contribution from the bulk -CH$_2$-CH$_2$- network does not depend on hydration level, hence information related to its position, line width, and percentage needs to be known in order to estimate *p* and for further analysis of the spectral contributions of bulk water and surface protons in PMO$_E$. In order to extract approximately the dipolar-broadened proton line shape associated with the –CH$_2$-CH$_2$- protons, a two dimensional ^{1}H-^{13}C wide-line separation experiment was performed at 10 kHz MAS with a short cross polarization contact time. The F$_1$ projection (SI **Fig. 1**) corresponding to the –CH$_2$-CH$_2$- ^{13}C resonance (~5ppm) provided a broad peak centred at ~2 ppm with a FWHM of ~3200 Hz. This information was utilized when calculating the total integrated intensity of the bulk water and surface protons.
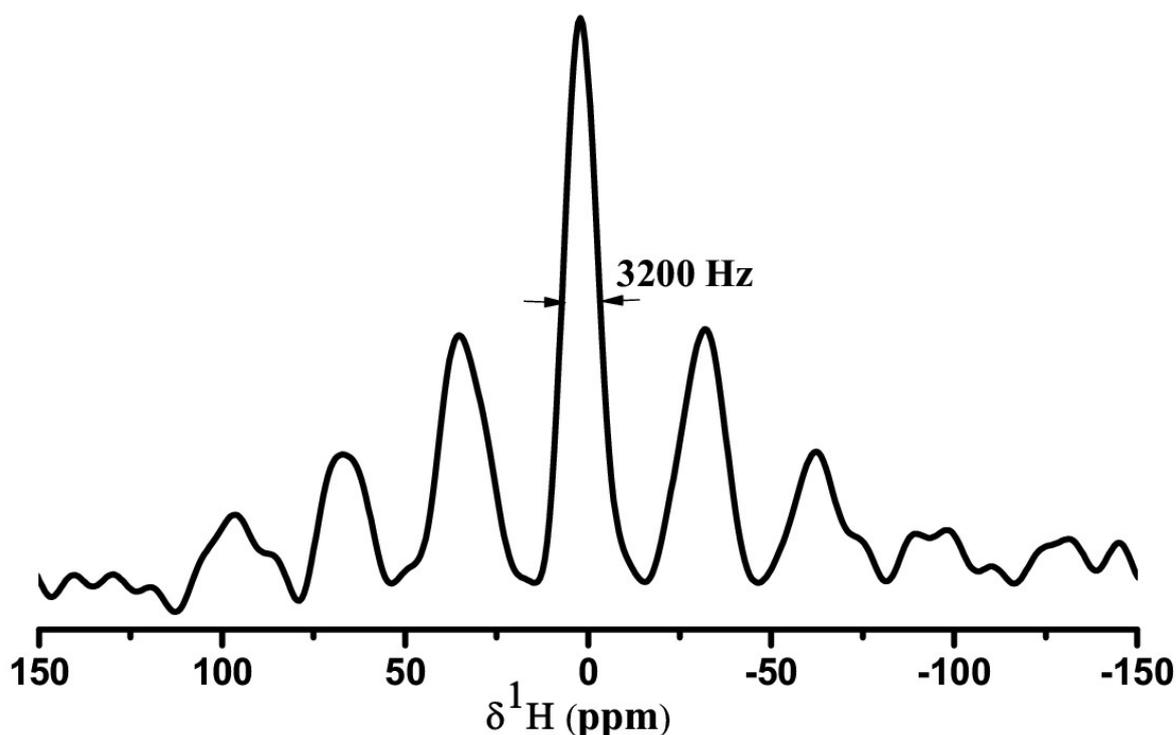
SI-Fig. 1: Proton F$_1$ projection extracted from a 2D Wide-line Separation spectrum acquired at 10 kHz MAS with a DSX 300 MHz spectrometer at room temperature. The centreband is positioned at 2 ppm, with a FWHM of ~3.2 kHz. The projection is extracted at the maximum of the ^{13}C resonance (5.3 ppm).

Deconvolution of the PMO$_E$ proton spectrum

The projection extracted from the two dimensional wide-line MAS spectrum shown in **SI-Fig.1** was used to estimate the line width and position of the resonance associated with the –CH$_2$-CH$_2$ protons in the PMO$_E$ bulk. The proton centreband is located at 2 ppm with a full width at half maxima (FWHM) of ~3200 Hz. Subsequently, the 1D proton spectrum corresponding to the driest state, with p~3H/nm^2, of the PMO$_E$ sample has been deconvoluted by incorporating, besides the bulk water and surface proton components, a component centred at ~2ppm and FWHM of ~3200 Hz whose amplitude was optimized, together with the amplitudes and lines widths of all the other components, to get the best fit model. The proton spectrum of the driest state of the sample has been selected for optimization because the spectral intensity due to –CH$_2$-CH$_2$-is significant in this case due to less percentage of bulk water and surface protons. Since the amount of –CH$_2$-CH$_2$ protons is constant in the sample at all hydration levels, all PMO$_E$ spectra are deconvoluted by incorporating the broad lineshape component with the same position, amplitude, and linewidth determined for the driest sample. In all deconvolutions, the broad dipolar lineshape at 2ppm is referred as the 'base'. The spectrum with the best fit at p~3 H/nm^2 is shown below.
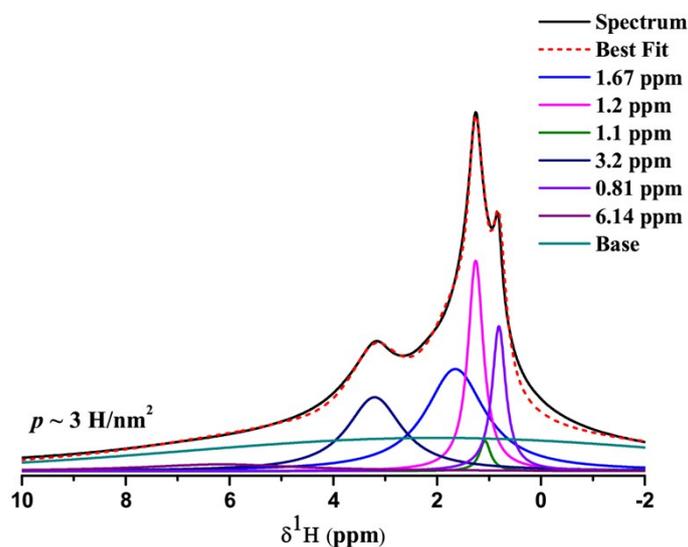
SI-Fig. 2: Deconvolution of proton MAS spectrum of PMO$_E$ at p~3 H/nm^2 using DMFIT.
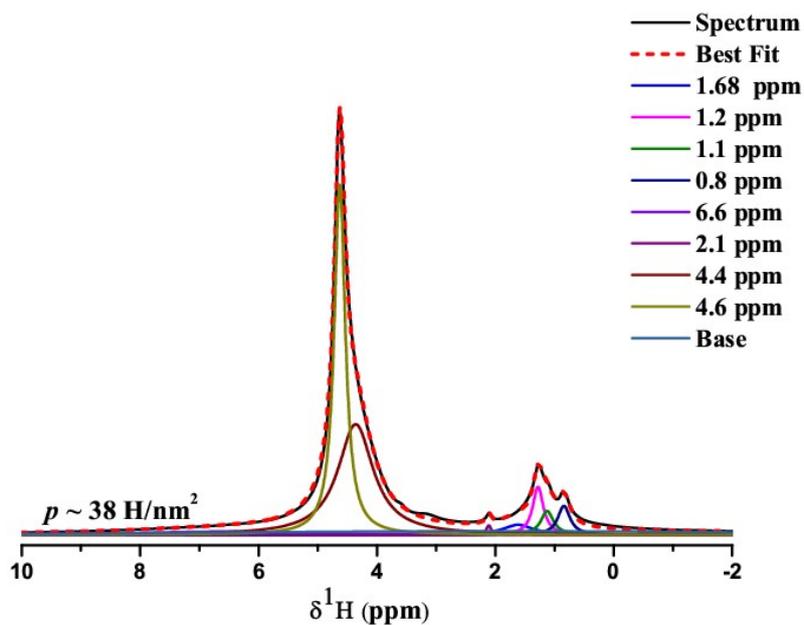
p (H/nm^2)	1.62 ppm (%)	1.13ppm (%)	4.4 ppm (%)	4.63 ppm (%)	6.59 ppm (%)
38	3.6	3.5	50.4	34.8	7.7

SI-Fig. 3: Deconvolution of proton MAS spectrum of PMO$_E$ at $p \sim 38$ H/nm^2 using DMFIT. The corresponding chemical shifts including the impurities (2.1 ppm (~0.2%), 1.2, 0.8 ppm) are indicated along with the best fit.
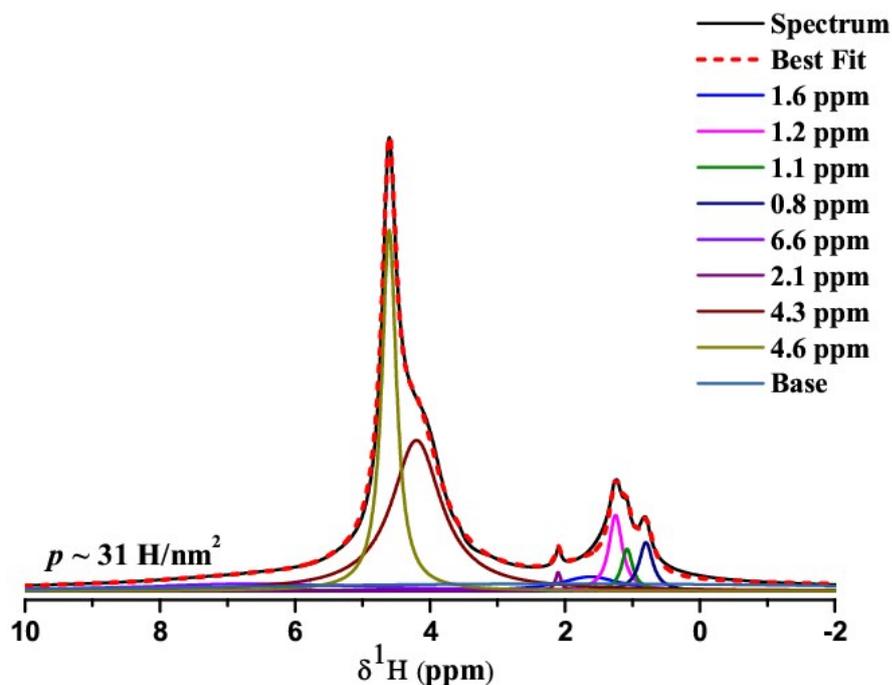
| p | 1.63 ppm | 1.1 ppm | 4.3 ppm | 4.6 ppm | 6.6 ppm |
(H/nm²)	(%)	(%)	(%)	(%)	(%)
31	5.3	3.2	48.3	34.9	8.3

SI-Fig. 4: Deconvolution of proton MAS spectrum of PMO_E at $p \sim 31$ H/nm² using DMFIT. The corresponding chemical shifts including the impurities (2.1 ppm (~0.2%), 1.2, 0.8 ppm) are indicated along with the best fit. The percentages of the relative integrated intensity after subtraction of the impurity peaks are given.
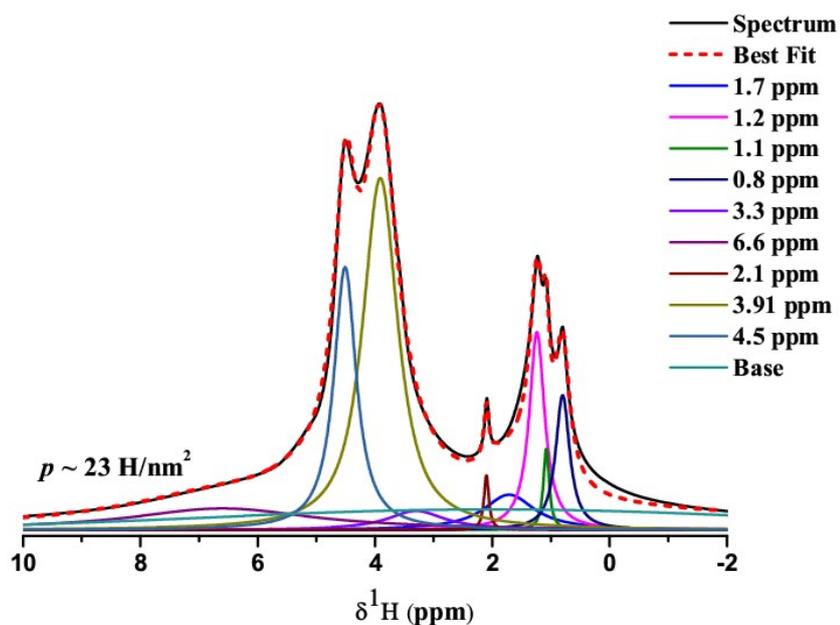
p (H/nm^2)	1.71 ppm (%)	1.06 ppm (%)	3.3 ppm (%)	3.91 ppm (%)	4.51 ppm (%)	6.6 ppm (%)
23	7.2	3.9	4.4	48.7	24.4	11.4

SI-Fig. 5: Deconvolution of proton MAS spectrum of PMO$_E$ at $p \sim 23$ H/nm^2 using DMFIT. The corresponding chemical shifts including the impurities (2.1 ppm (~0.2%), 1.2, 0.8 ppm) are indicated along with the best fit. The percentages of the relative integrated intensity after subtraction of the impurity peaks are given.
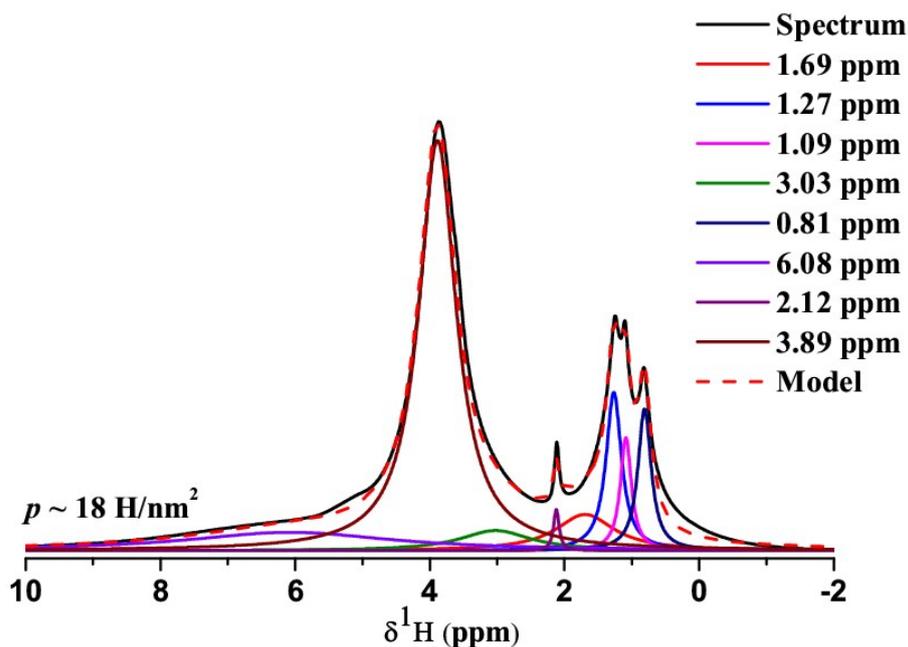
p (H/nm^2)	1.64 ppm (%)	1.1 ppm (%)	3.3 ppm (%)	3.9 ppm (%)	6.08 ppm (%)
18	11.2	3.0	4.5	66.7	14.6

SI-Fig. 6: Deconvolution of proton MAS spectrum of PMO$_E$ at $p \sim 18$ H/nm^2 using DMFIT. The corresponding chemical shifts including the impurities (2.1 ppm (~0.2%), 1.2, 0.8 ppm) are indicated along with the best fit. The percentages of the relative integrated intensity after subtraction of the impurity peaks are given.
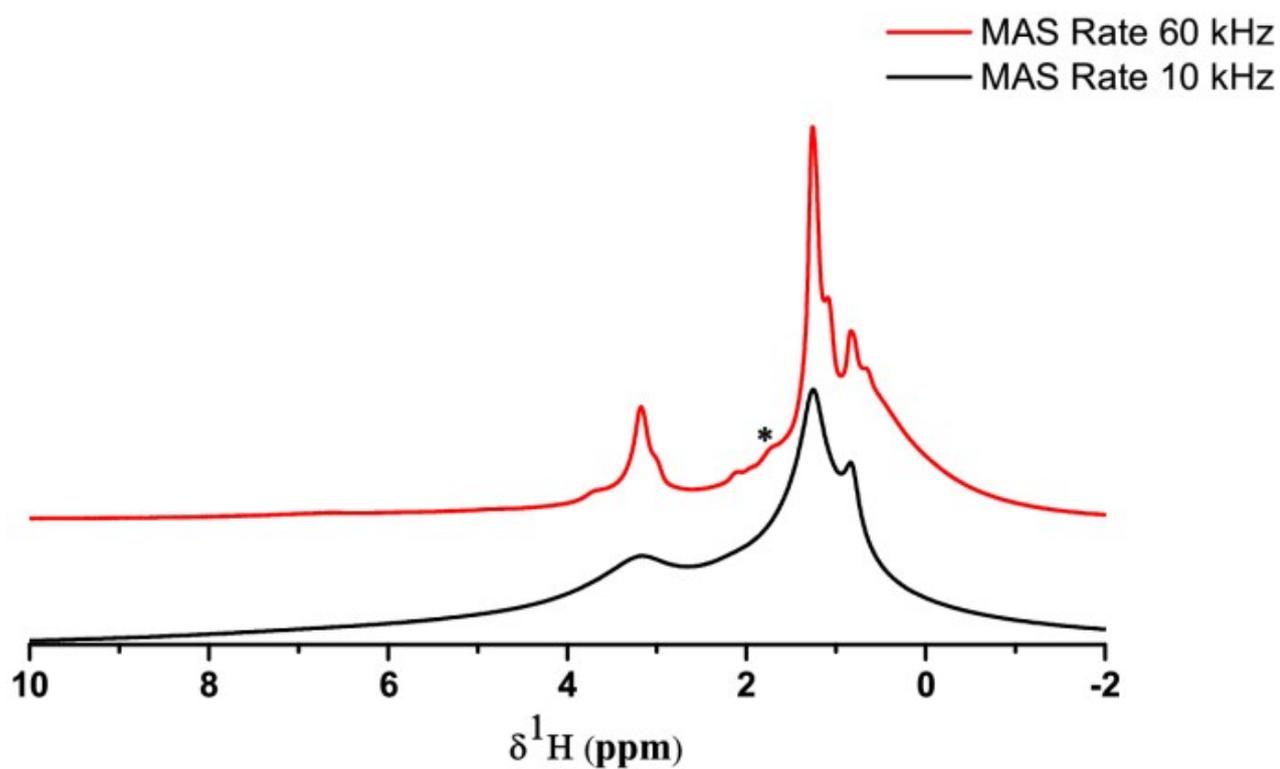
SI-Fig. 7: Proton MAS spectrum of PMO_E at $p \sim 3$ H/nm^2 recorded at MAS rates of 60 kHz (red) in a 700 MHz spectrometer and 10 kHz (black) in a 300 MHz spectrometer. The proton resonance corresponding to 1.7 ppm is marked by (*).
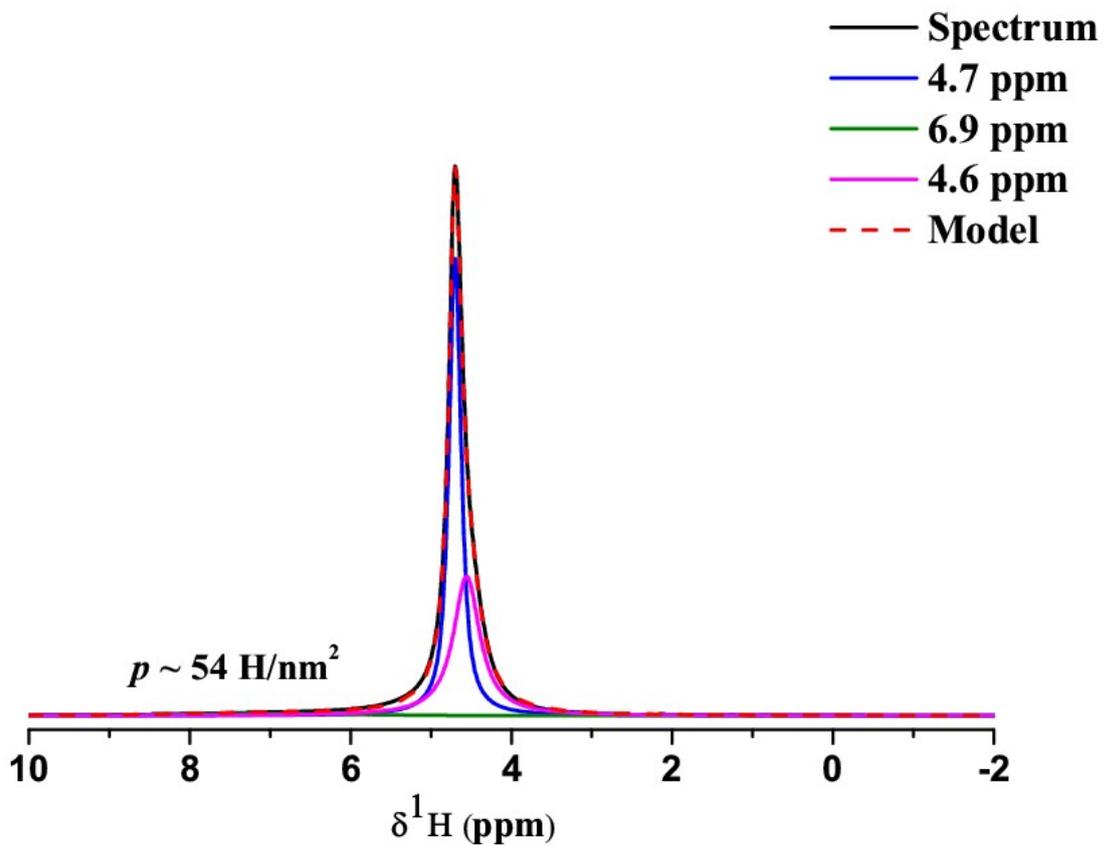
p (H/nm²)	4.6 ppm (%)	4.4 ppm (%)	6.9 ppm (%)
54	57	40	3

SI-Fig. 8: Deconvolution of proton MAS spectrum of SBA-15 at $p \sim 54$ H/nm² using DMFIT.
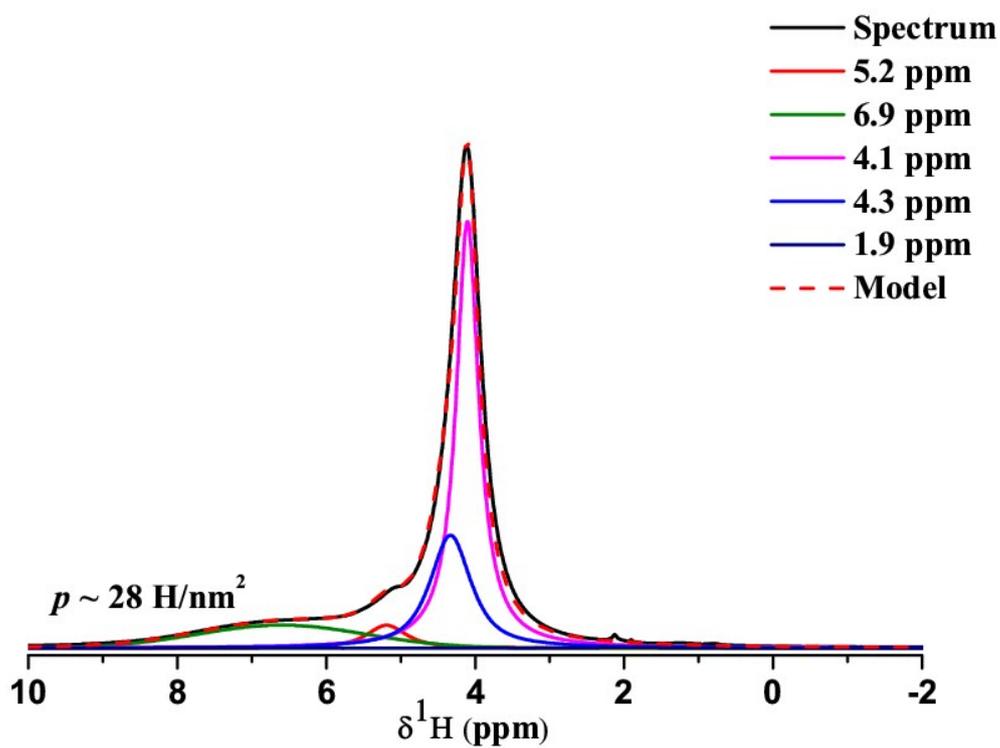
| p | 1.9 ppm | 4.1ppm | 4.3 ppm | 5.2 ppm | 6.9 ppm |
(H/nm²)	(%)	(%)	(%)	(%)	(%)
28	0.5	55.5	24.5	4.8	14.7

SI-Fig. 9: Deconvolution of proton MAS spectrum of SBA-15 at $p \sim 28$ H/nm² using DMFIT.
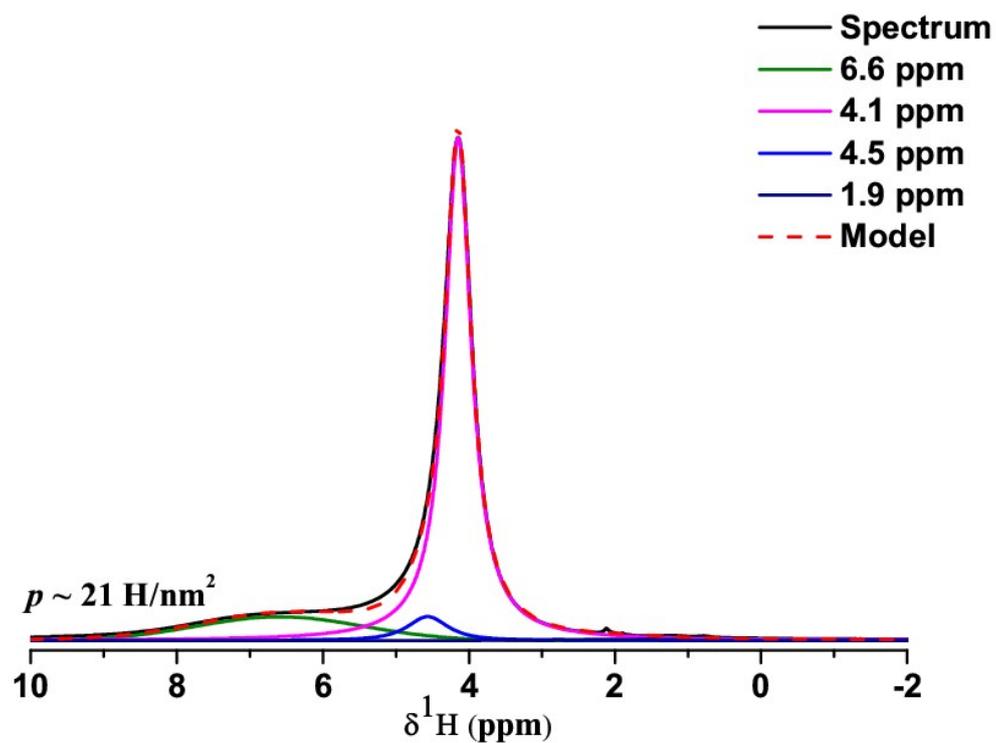
p (H/nm^2)	1.9 ppm (%)	4.1 ppm (%)	4.5 ppm (%)	6.6 ppm (%)
21	0.8	78.5	5.3	15.4

SI-Fig. 10: Deconvolution of proton MAS spectrum of SBA-15 at $p \sim 21$ H/nm^2 using DMFIT.
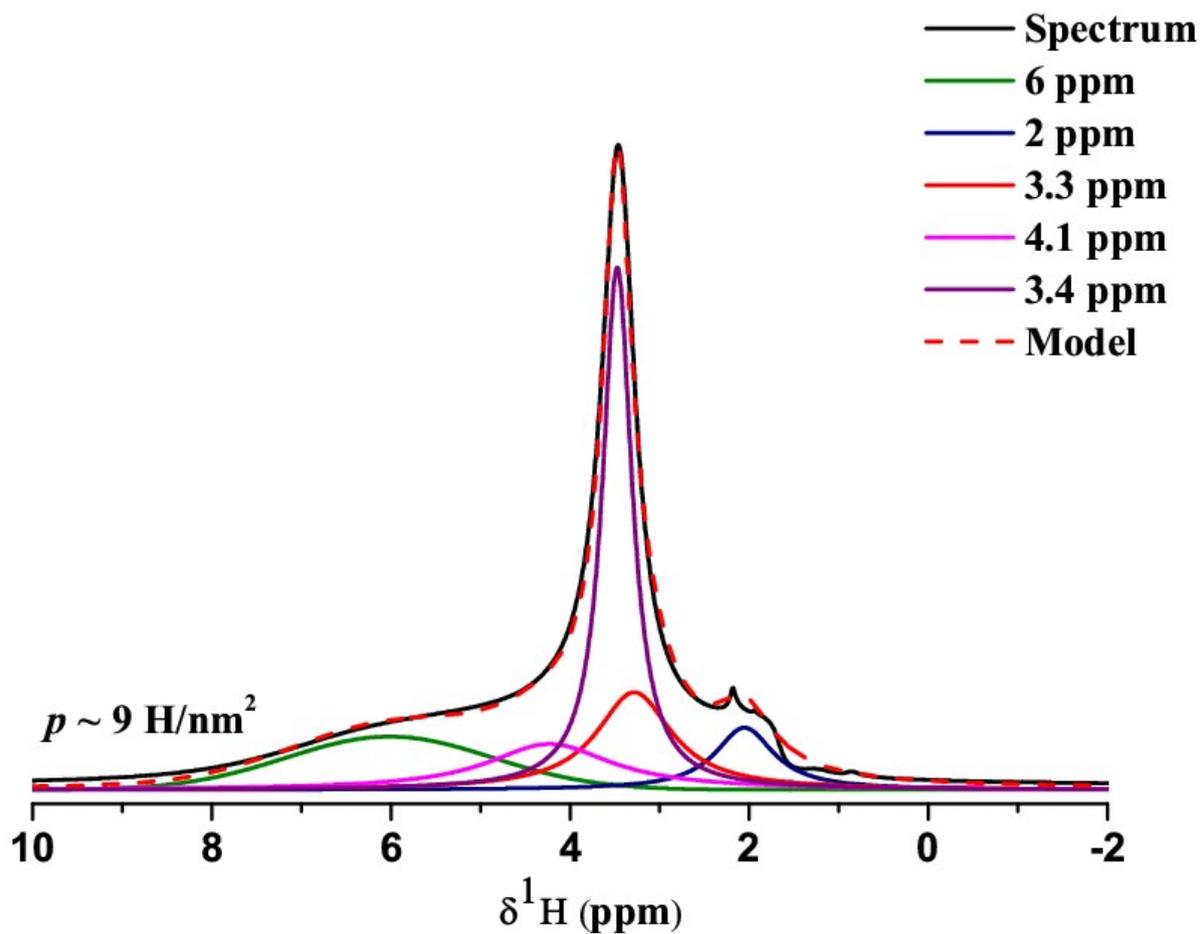
p (H/nm^2)	2 ppm (%)	3.3 ppm (%)	3.4 ppm (%)	4.1 ppm (%)	6 ppm (%)
9	9.3	18.7	39	14.6	18.4

SI-Fig. 11: Deconvolution of proton MAS spectrum of SBA-15 at $p \sim 9$ H/nm^2 using DMFIT.